The upgraded Collective Thomson Scattering diagnostics of FTU

W. Bin[a], A. Bruschi[a], O. D'Arcangelo[b], G. Grosso[a], L. Lubiako[c], U. Tartari[a], L. Figini[a], S. Garavaglia[a], G. Grossetti[d], A. Moro[a], F. Orsitto[b], C. Centioli[b], C. Galperti[a], G. Granucci[a], V. Mellera[a], D. Minelli[a], A. Nardone[a], A. Simonetto[a], M. Vellucci[b]

[a]*Istituto di Fisica del Plasma - CNR, Milano, Italy*
[b]*ENEA Unità Tecnica Fusione, C.R. Frascati, Frascati (Roma), Italy*
[c]*Institute of Applied Physics - RAS, Nizhny Novgorod, Russia*
[d]*Institute for Applied Materials - KIT, Karlsruhe, Germany*

The 140 GHz Collective Thomson Scattering (CTS) diagnostics installed on the Frascati Tokamak Upgrade (FTU) has been upgraded. The new system now is ready both to detect the thermal CTS radiation (for the first time with the probe frequency below the 1st harmonic electron cyclotron resonance) and to study the impact of possible parametric decay instability (PDI) processes on the received signals. The EC front-steering antenna and transmission system have been complemented with a receiving line that matches a quasi-optical line feeding the homodyne multi-channel radiometer. The scattering volume can be placed in a wide range of locations by means of fast poloidal and toroidal rotations of the two plasma-facing mirrors that have an up-down symmetry with respect to the equatorial plane of the torus. The data acquisition system has been improved adding a new digitizer, with a bandwidth of 5 GHz and a maximum sampling rate of 12.5 GS/s. The possibility of directly sampling and Fourier transforming the down-converted signals greatly improves the suitability of the new diagnostics to carry out thermal ion temperature measurements and to study the competing PDI processes whenever present.

Keywords: collective scattering; electron cyclotron waves; parametric decay instability; radiometric systems.

1. Introduction

During the last two years the Collective Thomson Scattering (CTS) diagnostic installed on the Frascati Tokamak Upgrade (FTU) device, operating at the frequency of 140 GHz, has been upgraded. The new system allows to detect the thermal scattering signal using a high power probe gyrotron frequency that can be also below the 1st harmonic electron cyclotron resonance, as previously attempted only in the low-power experiment in TFTR [1]. This goal was the same already prefixed with the previous CTS system installed in FTU [2, 3], which operated for several years with a completely different optical configuration, before being decommissioned due to critical issues found during the experiments, as described in [4]. These criticalities were related to a positioning of the launching mirror too close to the EC harmonic resonance layer when operating with the CTS configuration at high magnetic field and to the material of the mirror (made of stainless steel, reaching very high temperature during the pulse). They are not found in the present launching system with a front-steering copper mirror in a more favorable position in the port. Now the diagnostic allows also the study of particular kinds of strong anomalous signals appearing in the spectra. Such signals, characterized by rapidly modulated non-linear power scaling with the plasma parameters, have been newly discovered with the CTS diagnostics of other tokamak [5, 6] and seem to be correlated with the presence of magnetic islands in the plasma. According to the theoretical models, the occurrence of this kind of signals should be ascribed to a parametric decay instability (PDI) process occurring in particular conditions that strongly lower the probing power threshold for PDI [7, 8] with respect to the one predicted by previous models. The impact of the PDI on the launched millimeter-wave beam as well as on the received signals is worth being studied in detail since the presence of strong additional emissions may limit the use of CTS, either when used to diagnose thermal ions or in ITER, where it will be mainly focused on the study of the fast ion distribution function [9]. Finally, as a third aim, the new system has been designed for the detection of fluctuation signals coherent with fast MHD phenomena, like rotating tearing modes, and for the measure of signals originating in overdense plasma regions through mode conversion processes [10-12].

2. The new transmission line

FTU offers the possibility to test the collective scattering in conditions of density and probe beam injection similar to those envisaged for the CTS fast ion diagnostic in ITER [13]. Either the ordinary or the extraordinary propagation mode can be chosen for the 500 kW probe beam, which is provided by a GYCOM gyrotron operating at 140 GHz. The new antenna system [14, 15] is provided with two symmetrical lines with a front-steerable mirror each. One of these lines (line-1, the upper one) has been designed in such a way that it can be dedicated either to EC power injection or to the detection of signals. These two different uses can be easily commuted from shot to shot [16]. As shown in Fig. 1-left, a quasi-optical box (switch L1/NL) mounted outside the cryostat and containing a flat movable mirror, allows deviating the radiation coming from the gyrotron between the old pre-existing ECRH launcher (L1) and the new launcher (NL). A second similar box (switch

author's email: wbin@ifp.cnr.it

ECRH/CTS) allows changing the connection of the NL between the gyrotron transmission line (ECRH) and the new receiving line (CTS), recently installed. Both the switches are pneumatic and can be remotely controlled. When the antenna is commuted to CTS operation the radiation is deflected to a new set of five quasi-optical boxes (Fig. 1-right) through a mitre-bend and a section of HE_{11} overmoded corrugated waveguide with a diameter of 88.9 mm. These mirror boxes connect the upper line of the antenna (and the new section of the CTS line) with a pre-existing quasi-optical transmission line that drives the radiation to the homodyne radiometric receiver.

3. The scattering geometry

The new CTS configuration (Fig. 2) is such that the probe beam and the detected signal directions have an up-down symmetry with respect to the equatorial plane of the tokamak. Fig. 2-right shows a poloidal view of a beam tracing calculation, carried out with the GRAY code [17], for a probe beam (red), launched from the lower line of the antenna, crossing at the plasma center the receiving beam (blue), detected from the upper line. In the simulations the beam edges are at the radius where the intensity drops to $1/e^2$ of its axial value. This simulation has been performed using the plasma parameters of shot #33373 (B_T=4.7 T, I_P=500 kA), where the resonant layer (5 T) for the 140 GHz frequency is in the plasma. In this case the probe beam power is absorbed and a strong electron cyclotron signal is emitted from the plasma. Despite they are unsuited to perform ion temperature measurements due to the strong ECE, when the aim of the investigation are the signals produced by PDI processes, the configurations with the resonant layer within the plasma become viable, these signals being expected to be considerably stronger than ECE. They are also of great interest due to the possibility they offer of comparing the resonant and non-resonant cases. The positions of the q=2 and q=3/2 surfaces are indicated in the picture, where typically magnetic islands develop in presence of Neon induced MHD activity. The new antenna allows moving the scattering volume on both these resonant surfaces, allowing studying the anomalous PDI signals originating from magnetic islands. A similar simulation is shown in three dimensions in Fig. 3, for shot #34166 (B_T=7.2 T, I_P=500 kA), where the scattering volume is at high toroidal angle (~35°). Such a high field configuration, where the probe gyrotron frequency is below the 1st harmonic EC resonance in the entire plasma volume, is reachable only in FTU and can be exploited to carry out non-resonant CTS measurements in the same conditions of ITER. The position of the resonant layer is not shown in this simulation since it is outside the plasma. The incident ($\mathbf{k}_i$) and the scattered ($\mathbf{k}_s$) wave vectors define $\mathbf{k}_{cts}$ (Fig. 3-right), the vector that gives the direction on which the three-dimensional ion velocity distribution $f(\mathbf{v})$ must be projected to obtain the mono-dimensional distribution $\Phi(v_p)$ resolved by CTS measurements: $\Phi(v_p)=\int f(\mathbf{v})\delta\left(v_p-\frac{\mathbf{k}_{cts}\cdot\mathbf{v}}{|\mathbf{k}_{cts}|}\right)d\mathbf{v}$, where v_p is the velocity component along the direction $\mathbf{k}_{cts}/|\mathbf{k}_{cts}|$ and δ is the Dirac delta function. The dynamical flexibility of the antenna allows varying the position of the scattering volume either on the equatorial plane or out of it. Both the scattering angle $\vartheta=arccos\frac{\mathbf{k}_i\cdot\mathbf{k}_s}{|\mathbf{k}_i||\mathbf{k}_s|}$ and the magnetic angle $\phi=arccos\frac{(\mathbf{k}_s-\mathbf{k}_i)\cdot(\mathbf{B}_{tor}+\mathbf{B}_{pol})}{|\mathbf{k}_s-\mathbf{k}_i||\mathbf{B}_{tor}+\mathbf{B}_{pol}|}$ can be changed during the shot, with fast angular movements of the two steerable mirrors, and great flexibility is permitted in the choice of the trajectories to follow with both the probe beam and the line of sight. The angles ∇ and ϕ are shown in Fig. 3-right. ~~The scattering volume is here considered to be the region limited by the surface at $(1/e)^{1/2}$ of the overlap function (i.e. the product function of the electric fields of the two beams). The spatial resolution, respectively on the direction of $\mathbf{k}_{cts}$ and on the other two orthogonal directions, is 133 mm / 50 mm, for the maximum toroidal injection/detection angle of 35°, and 47 mm / 25 mm, for a typical low toroidal angle of 5°.~~ The scattering volume is here considered to be the region limited by the surface at 1/e of the overlap function (i.e. the product function of the electric fields of the two beams), from which 74% of the power is scattered. The spatial resolution, respectively on the direction of $\mathbf{k}_{cts}$ and on the other two orthogonal directions, is 191 mm / 71 mm, for the maximum toroidal injection/detection angle of 35°, and 67 mm / 35 mm, for a typical low toroidal angle of 5°. The $\mathbf{k}$-resolution is calculated following reference [18] but retaining the full expressions in the scattering angle ∇, being the small angle limit considered in the reference not applicable to the CTS geometry in FTU. The resolution $\Delta\mathbf{k}/\mathbf{k}_{cts}$ ranges from $0.3\cdot10^{-2}$ to $1.0\cdot10^{-2}$, in the direction of $\mathbf{k}_{cts}$, and from $0.9\cdot10^{-2}$ to $2.2\cdot10^{-2}$, in the orthogonal plane, depending on the toroidal injection/detection angle (with smaller values for larger toroidal angles). Wide angular ranges in toroidal and poloidal directions can be scanned with the mirrors. In particular, the scattering volume can be moved toroidally from the perpendicular position in front of the antenna up to high angles, in both positive and negative directions. This allows varying considerably the angle ϕ, from which the scattering signals strongly depend. The range $0^\circ<|90^\circ-\phi|<50^\circ$ approximately holds true when scattering is detected at the plasma center. The angle ϕ increases as the radiation is scattered away from the toroidal field direction and modulations at the ion cyclotron frequency ω_{ci} appear in the detected spectra as ϕ approaches 90°. In our case the large range of toroidal angles available with the FTU antenna allows studying either CTS spectra strongly modulated by the ion gyro-motion or spectra in almost complete absence of ion cyclotron structures.

4. Polarization control

Polarization control of the received beam, absent in the old CTS system, has been introduced. A universal polarizer, made with two corrugated mirrors (one with

λ/4 and one with λ/8 corrugation depth) has been placed at the end of the quasi-optical transmission line, before the receiving horn, allowing to measure the total power coupling either in the ordinary or in the extraordinary mode. The final part of the line was rearranged to preserve the optical beam path. The correct orientation of the polarizers has been defined with low power measurements. A dedicated numerical code has been also developed for this aim. The code is capable to calculate step by step the changes of the beam polarization along the CTS line, from the plasma to the radiometer, considering the entire beam path through the FTU antenna as well as through the new and the pre-existing sections of transmission line.

5. The radiometric and acquisition system

The receiver is a homodyne radiometer with central frequency of 140 GHz. In the system used up to now (still installed and operating) the spectra are resolved by a multichannel spectrum analyzer with 32 channels of progressively increasing width ($\Delta f_n = f_{0n}/10$, where f_{0n} is the central frequency of the n^{th} channel), capable to provide a single-sideband detection in the band 50-1200 MHz around the local oscillator frequency, that for the thermal CTS measurements is usually tuned at the gyrotron frequency. After ~25 ms from the beginning of the pulse, in which it has a shift of ~50 MHz, the gyrotron frequency becomes stable in a frequency range of +/-5 MHz. To protect the mixer during the frequency drift a pin diode is used to blind the receiver for the proper time interval. The radiometric sensitivity of this system is in the range 0.05-1 eV, depending on the channel. The data acquisition and analysis system has been recently improved with the addition, in parallel, of a new digitizer with a bandwidth of 5 GHz and a maximum sampling rate of 12.5 GS/s. With this system the reconstruction of the scattered radiation spectra is obtained by direct sampling of the down-converted signal, which can be directly Fourier transformed shot by shot. This ensures the suitability of the new FTU diagnostic to study the anomalous PDI signals, for which an acquisition speed suitable for the fast changes due to rotating magnetic islands is required.

6. The TCSC code

A new code, named TCSC (Thermal Collective Scattering Code), has been developed at IFP/CNR in support to the CTS experiment. The code relies on a basic physical model [19-20], where the probe beam is scattered by electron density fluctuations due to the ion motion. The fluctuations of different kinds that more refined theoretical models (e.g., see [21]) predict to affect the spectra in particular conditions will accordingly manifest themselves as difficulties in best-fitting the spectral data, so indirectly proving an insight on the presence of these additional effects not described by the model adopted in the code. TCSC is capable either to predict the CTS spectra to be expected for a given set of input parameters, when used in predictive mode, or to infer a number of plasma parameters (first of all the local ion temperature) by best fit of an input spectrum, when used in interpretative mode. Consistently with the aim to demonstrate the measurability of the local ion temperature, Maxwellian ion velocity distributions are assumed in the computations. The description of the plasma in the magnetized approximation allows the computations to be extended to the conditions where the spectra become modulated at the ion cyclotron frequency. ~~Several non-linear least-squares methods [22] are exploited to best fit the spectra with up to five free parameters. Three of them, the ion temperature and the local concentrations of (up to) two impurity species, have direct physical interest. The inclusion of an impurity contribution in the model function provides a check of the actual presence of the impurity in the plasma, since such inclusion improves the best fitting if the impurity is effectively present but worsen it in the opposite case. While more complicated dependences of the spectra from the relevant parameters might result from more refined models, such as [21] and related references contained therein, according to the model [19, 20] used in the TCSC code, only information about the product $z_i \cdot C_i$, where z_i and C_i are respectively the strip number and the concentration of the impurity, can be obtained from the spectral data. Information on the local concentration C_i is obtained in this case whenever the strip number of the impurity involved is known. If not, the information obtained with the code simulations concerns only the product $z_i \cdot C_i$.~~ Several nonlinear least-squares methods [22] are exploited to best-fit the spectra with up to five free parameters, three of which (the ion temperature and the local concentrations of up to two impurity species) of direct physical interest, using the model function for a multi-species plasma referred to in [19-20]. Despite possible uncertainties related to the non uniqueness of the solutions, the best-fitting performance, hence the estimate of the ion temperature itself, will turn out to be optimized, for a given number of free parameters, when the guessed impurity species and charge state(s) correspond to those effectively present in the plasma, provided they are such as to appreciably affect the spectrum. TCSC is organized to operate interactively and it is thought to operate either with real FTU data (predictive mode) and spectra (interpretative mode), or with dummy data and spectra simulating the real ones. In particular, besides returning the spectrum shape expected for a given set of real FTU data (predictive mode), the code allows to check the best-fitting performance to be expected for dummy spectra, ~~giving the possibilities to add an arbitrary amount of random noise~~ giving the possibility to add arbitrary amounts of random noise, to consider a number of perturbed channels and/or to exclude possible unreliable or out-of-duty channels (interpretative mode). It is worth mentioning that, in addition to their channel-integrated form, the code provides the underlying best-fitted spectra in full form. The smooth spectra being unaffected by the integrations, any difference between these two forms will be a signal of the insurgence of the modulations, which accordingly will be detectable even at small modulation depths. Two examples of spectra calculated with TCSC are shown in Fig. 4. The shown spectra are simulated for two different couples of angles, (ϑ, ϕ)=(135°, 66°) and (ϑ, ϕ)=(127°,

87°), and for two different ion temperatures. The simulations (where no integration is performed to take into account the finiteness of the scattering volume and the spread in the fluctuation wave-vector) give evidence that the modulations of the scattering function $S[\mathbf{k}, \omega]$ due to the ions gyro-motion are present only in the case of high magnetic angle ϕ=87°, while they already completely disappear for ϕ=66°, since this phenomenon gradually fades as the magnetic angle moves away from 90° (in both positive or negative directions). The estimate of the ion temperature provided by the TCSC code relies on the shape of the spectral data, independently of their amplitude. This explains why the polarization of the probe and received beams are neglected, being basically non-influential, or at worst such to modify only slightly the shape of the scattering function, in the range of the FTU parameters. The possibility available in FTU to access also regimes with spectra which are deeply affected by ion cyclotron structures can open the way to further extensions of the potential of CTS diagnostic [23].

Acknowledgments

The authors are very grateful to Dr Alexander Shalashov for the management of the support activity carried out by IAP/RAS.

References

[1] J.S. Machuzak, P.P. Woskov and J. Gilmore, Results from the low-power 60 GHz gyrotron collective Thomson scattering diagnostic on TFTR, Rev. Sci. Instrum. **68**, (1997) 458-461

[2] U. Tartari, G. Grosso, G. Granucci, F. Gandini, S. Garavaglia, G. Grossetti, et al., Evolution of the millimeter-wave collective Thomson scattering system of the high-field tokamak Frascati Tokamak Upgrade, Rev. Sci. Instrum. **78**, (2007) 043506

[3] F. Orsitto, A. Brusadin, Yu. Brodsky, S. Filchenkov, G. Grosso, E. Giovannozzi, et al., Characterization and preliminary results of the collective Thomson scattering system on FTU tokamak, Rev. Sci. Instr. **70**, (1999) 1158

[4] U. Tartari, G. Grosso, G. Granucci, L.V. Lubyako, A.G. Shalashov, E.V. Suvorov, et al., Critical issues highlighted by collective Thomson scattering below electron cyclotron resonance in FTU, Nucl. Fusion **46**, (2006) 928-940

[5] E. Westerhof, S.K. Nielsen, J.W. Oosterbeek, M. Salewski, M.R. De Baar, W.A. Bongers, et al., Strong Scattering of High Power Millimeter Waves in Tokamak Plasmas with Tearing Modes, Phys. Rev. Lett. **103**, (2009) 125001

[6] S.K. Nielsen, M. Salewski, E. Westerhof, W. Bongers, S.B. Korsholm, F. Leipold, et al., Experimental characterization of anomalous strong scattering of mm-waves in TEXTOR plasmas with rotating islands, Plasma Phys. Control. Fusion **55**, (2013) 115003 (11pp)

[7] E.Z. Gusakov and A.Yu. Popov, On the possibility of low-threshold anomalous absorption in tokamak 2nd-harmonic electron cyclotron resonance heating experiments, Europhys. Lett. **99**, (2012) 15001

[8] A.Yu. Popov, E.Z. Gusakov and A.N. Saveliev, On the low-threshold parametric mechanism of the anomalous power absorption in electron cyclotron resonance heating experiments in toroidal devices, JETP Lett. **96**, (2012) 164-70

[9] M. Salewski, S.K. Nielsen, H. Bindslev, V. Furtula, N.N. Gorelenkov, S.B. Korsholm, et al., On velocity space interrogation regions of fast-ion collective Thomson scattering at ITER, Nucl. Fusion **51**, (2011) 083014 (10pp)

[10] W. Bin, E. Alessi, A. Bruschi, O. D'Arcangelo, L. Figini, C. Galperti, et al., Antenna system analysis and design for automatic detection and real-time tracking of electron Bernstein waves in FTU, JINST **9**, (2014) P05001

[11] W. Bin, A. Bruschi, O. D'Arcangelo, C. Galperti, G. Granucci, A. Moro, et al., Feasibility study of O-X coupling for overdense plasma heating through O-X-B mode conversion in FTU, Nucl. Fusion **53**, (2013) 083020 (10pp)

[12] W. Bin, E. Alessi, A. Bruschi, C. Galperti, G. Granucci, G. Grossetti et al., A real-time tracking for optimal wave injection in overdense plasma heating experiments at 140 GHz in FTU, IEEE Trans. Plasma Sci. **40**, (2012) 622-628

[13] F.P. Orsitto, G. Giruzzi, A. Bruschi and W. Bin, Review of possibilities for a Collective Thomson Scattering diagnostic on tokamaks, 40th European Physical Society Conference on Plasma Physics, Espoo, Finland, (2013) P6.013

[14] W. Bin, A. Bruschi, S. Cirant, G. Granucci, S. Mantovani, A. Moro, et al., Design of a new ECRH launcher for FTU tokamak, Fusion Eng. Des. **84**, (2009) 451-456

[15] A. Bruschi, W. Bin, S. Cirant, G. Granucci, S. Mantovani, A. Moro, et al., A new launcher for real-time ECRH experiments on FTU, Fusion Sci. Technol. **55**, (2009) 94-107

[16] S. Garavaglia, E. Alessi, W. Bin, L. Boncagni, A. Bruschi, S. Cirant, et al., Installation, integration and power tests of the new fast ECRH launcher of FTU, Fusion Eng. Des. **88**, (2013) 998-1001

[17] D. Farina, A quasi-optical beam-tracing code for electron cyclotron absorption and current drive: gray, Fusion Sci. Technol. **52**, (2007) 154

[18] E. Holzhauer and J.H. Massig, An analysis of optical mixing in plasma scattering experiments, Plasma Phys. **20** (1978) 867

[19] I.H. Hutchinson, Principles of Plasma Diagnostics, Cambridge University Press (2002)

[20] J. Sheffield, Plasma Scattering of Electromagnetic Radiation, Academic, New York (1975)

[21] H. Bindslev, A quantitative study of scattering from electromagnetic fluctuations in plasmas, J. Atmos. Terr. Phys. **58**, (1996) 983-989

[22] P. Lindström and P.A. Wedin, Gauss-Newton based algorithms for constrained nonlinear least squares problems, University of Umea, S-901 87 Umea, Sweden, 1987, http://www8.cs.umu.se/~perl/reports/TEST/alg.pdf

[23] M. Stejner, M. Salewski, S.B. Korsholm, H. Bindslev, E. Delabie, F. Leipold, et al., Measurements of ion in neutral beam heated discharges at TEXTOR, Plasma

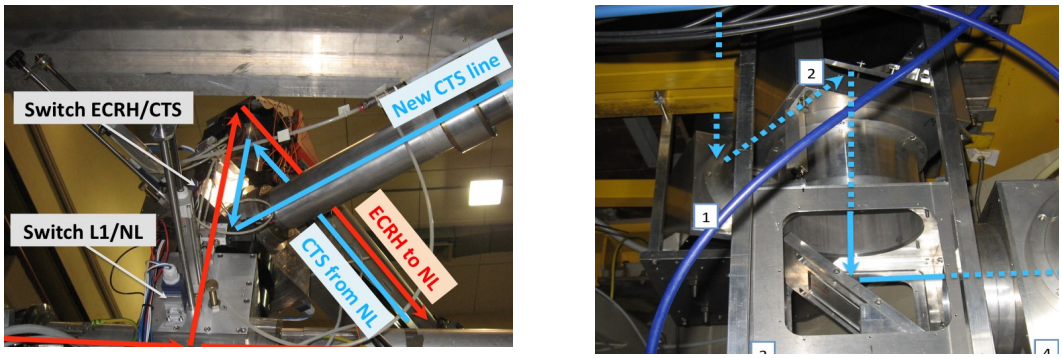

Fig. 1. Left: view of a section of the ECRH transmission line in the region around the switches L1/NL and ECRH/CTS of line-1. The new CTS receiving line is indicated with the blue arrow (top right). The waveguide above all the others can be used either for ECRH transmission to NL or for CTS reception from NL. Right: four of the quasi-optical boxes installed under the equatorial plane of FTU, connecting the new CTS receiving waveguide line to the pre-existing quasi-optical line. The blue arrows indicate the beam path in the boxes, from the plasma towards the radiometer.

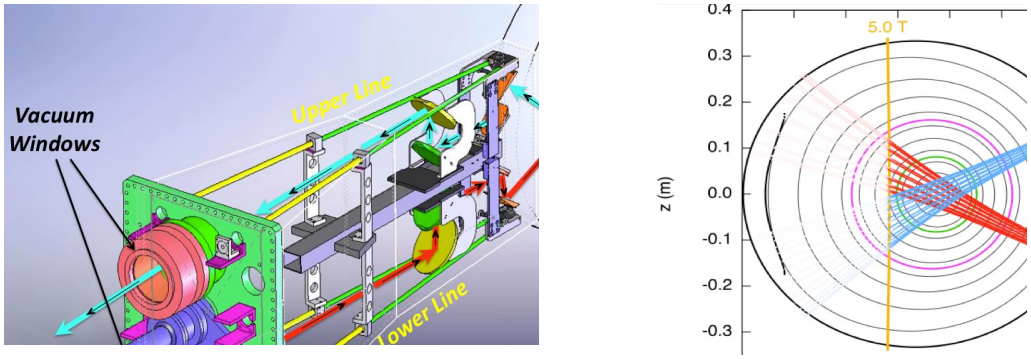

Fig. 2. A sketch of the new CTS configuration is shown on the left (picture taken and modified by [10]). The two symmetrical lines can be seen. The lower line of the antenna is used to inject the 140 GHz probe beam (red arrows) and the upper line, connected to the CTS line, is exploited to detect the scattered signal (light blue arrows). Right: beam tracing calculation of two beams crossing at the plasma center, in a configuration with the 5T resonant layer (shown with the vertical orange line) in the plasma. The positions of the q=2 (light purple) and q=3/2 (green) surfaces are indicated.

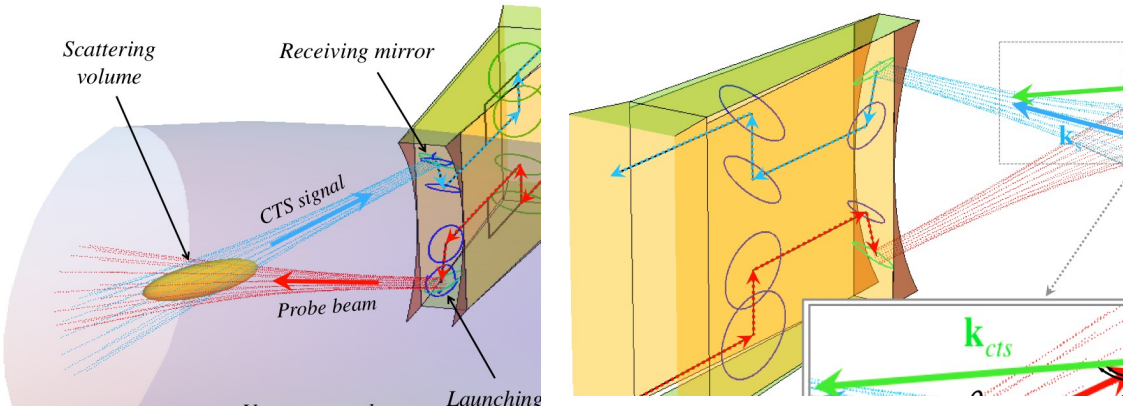

Fig. 3. Left: three-dimensional view of a beam tracing simulation of two beams crossing at high toroidal angle (~35°). The scattering volume and the steerable mirrors of the antenna are indicated. Right: the incident wave vector $\mathbf{k}_i$, the scattered wave vector $\mathbf{k}_s$ and $\mathbf{k}_{cts}=\mathbf{k}_s-\mathbf{k}_i$ are shown, together with the scattering angle $\nabla$and the magnetic angle ϕ□

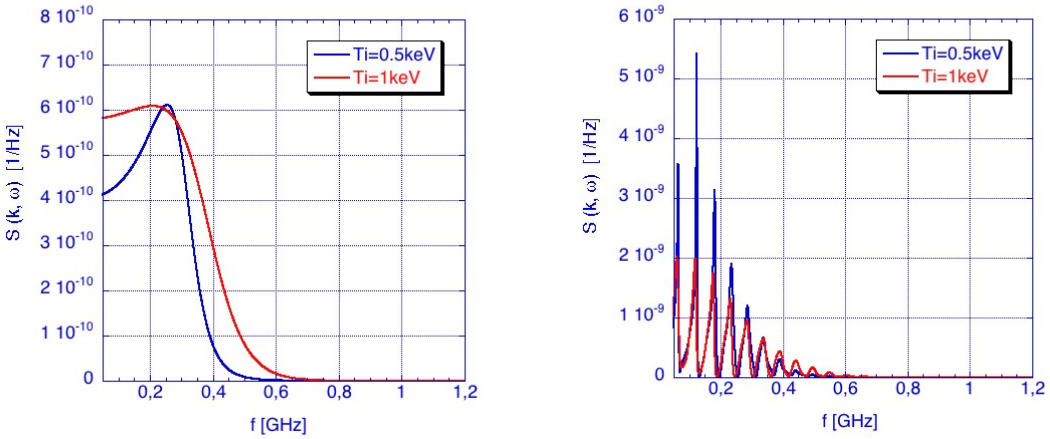

Fig. 4. Examples of spectra predicted with the code TCSC for the two couples of angles (ϑ, ϕ)=(135°, 66°), on the left, and (ϑ, ϕ)=(127°, 87°), on the right, and for two different ion temperatures. It can be noted that the ion cyclotron structures (strong modulation effect caused by the ion gyro-motion) are present only for magnetic angle near 90° (right figure), while they are absent for oblique measurements (left figure).